Actin-Binding Protein Requirement for Cortical Stability and Efficient Locomotion

C. CASEY CUNNINGHAM, JED B. GORLIN, DAVID J. KWIATKOWSKI, JOHN H. HARTWIG, PAUL A. JANMEY, H. RANDOLPH BYERS, THOMAS P. STOSSEL

Three unrelated tumor cell lines derived from human malignant melanomas lack actin-binding protein (ABP), which cross-links actin filaments in vitro and connects these filaments to plasma membrane glycoproteins. The ABP-deficient cells have impaired locomotion and display circumferential blebbing of the plasma membrane. Expression of ABP in one of the lines after transfection restored translocational motility and reduced membrane blebbing. These findings establish that ABP functions to stabilize cortical actin in vivo and is required for efficient cell locomotion.

FOR TWO CENTURIES BIOLOGISTS have inferred that protrusive activity, such as the pseudopod extension seen in locomotion, requires changes in the consistency of the cytoplasm of the cell periphery between gelled and fluid states (*1*). The molecular basis of these "sol-gel" transformations is thought to include the reversible assembly of monomeric actin into linear polymers and the organization of these filaments into membrane-bound three-dimensional networks. This actin network stabilizes (gels) the cell periphery and the attached plasma membrane. Protrusions from the cell surface of motile cells arise from destruction (solation) and reconstruction (gelation) of the actin filaments constituting this network. The actin-associated proteins, which regulate the assembly of actin into filaments and cross-link these filaments into three-dimensional gels in vitro (*2*), thus might influence cell surface activity and locomotion. However, genetic ablation from *Dictyostelium discoideum* amoebae of two proteins that cross-link actin filaments did not prevent protrusive activity or translocational locomotion of these cells (*3*), suggesting that some other proteins may have overlapping functions. In contrast, we now provide evidence that actin-binding protein (ABP), a homodimer with rodlike 280-kD subunits containing flexible hinges that allow cross-linking of dispersed actin filaments at wide angles (*4, 5*), is an essential component for stabilization of the cell surface, organization of protrusive activity, and efficient translocational locomotion.

Seven permanent cell lines derived from separate human malignant melanomas were separated into two groups on the basis of morphology and motility (*6*). Four of the lines, designated M4 to M7, are motile cells that have basal surface stress fibers and are dispersed before growing to confluence. The other three lines, designated M1 to M3, have no actin fiber bundles, grow in colonies, and show less random migration (*6*).

Immunoblotting or immunoprecipitation of Triton-soluble or Triton-insoluble cell extracts from lines M1 to M6 revealed that amounts of the actin-associated proteins gelsolin, α-actinin, profilin, and fodrin varied by no more than a factor of two between the six lines. However, ABP was undetectable in lines M1 to M3 when assayed by immunoprecipitation of detergent extracts (Fig. 1), immunoblotting of whole cell lysates, or immunostaining of fixed, permeabilized cells but was readily detectable in lines M4 to M6 by all of these assays (*7*). Furthermore, only small amounts of mRNA for ABP were detected by ribonuclease protection analysis in these lines M1 to M3. On Southern (DNA) blots, all six lines have identical patterns, indicating no gross alterations in ABP gene structure in the ABP-deficient (ABP^-) lines (*8*).

By light microscopy, cells from the ABP-containing (ABP^+) lines exhibit asymmetrical spreading to form lamellae that exclude organelles, whereas cells from the three ABP^- lines lacked such extensions (*9*). Cells from all ABP^- lines displayed extensive, continuous blebbing of the plasma cell membrane (Fig. 2). The blebs, which exclude visible organelles, ceased to appear if the ambient temperature of the cells fell below 30°C or after removal of serum, but resumed within 60 s if normal culture conditions were restored. In the presence of serum at 37°C, the ABP^+ lines manifested either ruffling or transient blebbing at one part of their periphery, typically at the leading edge of a migrating cell, and those blebs sometimes flattened and transformed into ruffling lamellae (Fig. 2).

To test whether the presence or absence of ABP accounted for the differences between these two groups of cells, we transfected ABP into cells from line M2 in a mammalian expression vector (LK444) containing full-length human ABP cDNA (LK-ABP) (*10*). As a control, cells (M2T) were transfected with the LK444 vector without the ABP cDNA insert. Seven clonal sublines of LKABP-transfected cells were isolated, designated M2A1 to M2A7. The molar ratio of ABP to actin varied in these cell lines as follows: M2T, <1:900; M2A1, 1:100; M2A2, 1:330; M2A3, 1:120; M2A4, 1:190; M2A5, 1:140; M2A6, 1:550; M2A7, 1:160 (Fig. 1). All of the cells within a given subline expressed ABP in similar amounts and expression of actin and other actin-associated proteins such as gelsolin, profilin, α-actinin, and fodrin was unchanged from controls.

Six of the seven ABP-transfected sublines had only transient localized blebbing resem-

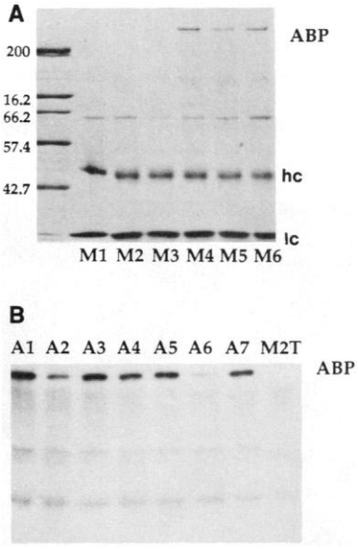

Fig. 1. ABP expression in the various cell lines. (**A**) Deficiency of ABP in M1–M3. Coomassie blue–stained SDS-polyacrylamide gel of proteins immunoprecipitated with antibody to ABP coupled to Sepharose beads from lysates of cell lines M1 through M6. The heavy (hc) and light (lc) chains of the antibody are also visible, as is a nonspecific band. Molecular size standards are marked. (**B**) Autoradiograph of an immunoblot of total cell protein (10 μg) from each of the seven ABP-transfected sublines (M2A1 to M2A7) and the control transfected line M2T. By scanning Coomassie-stained SDS-polyacrylamide gels of whole cell extracts with a laser densitometer (LKB Pharmacia, Piscataway, New Jersey), we estimate that actin makes up 11% of total cell protein in M2; this was not changed by transfection. After scanning band intensities and comparing them to known amounts of ABP on a separate blot, we estimated the molar ratio of ABP to actin for each cell line, allowing for the differences in molecular size. We also estimated the molar ratio of ABP to actin in the cell lines M4 (1:80), M5 (1:120), and M6 (1:140).

C. C. Cunningham, J. B. Gorlin, D. J. Kwiatkowski, J. H. Hartwig, P. A. Janmey, T. P. Stossel, Divisions of Experimental Medicine and Hematology-Oncology, Brigham & Women's Hospital, Department of Medicine, Harvard Medical School, Boston, MA 02115.
H. Randolph Byers, Department of Pathology, Massachusetts General Hospital, Boston, MA 02114.
J. B. Gorlin, Department of Hematology-Oncology, Children's Hospital, Pediatric Oncology Division, Dana-Farber Cancer Institute, Boston, MA 02115.

bling that of the native ABP$^+$ lines, and these cells also acquired greater general asymmetry in shape and focal lamellae that excluded organelles (Fig. 2). The M2A6 subline, which expressed the lowest amount of ABP, (molar ratio of ABP to actin, 1:550) had more extensive blebbing, with 30% of the cells showing circumferential blebbing at a given time. All of the sublines showed increased translocational motility when compared to the untransfected ABP$^-$ line (*11*). Up to five times more transfected cells than untransfected cells migrated through a porous membrane in response to a gradient of chemoattractant (Fig. 3), and motility increased in proportion to ABP expression up to a molar ratio of ABP to actin of 1:160, before declining somewhat when higher amounts of ABP were expressed. The molar ratios of ABP to actin associated with maximal migration in the transfected sublines are in the same range as those found in motile cells such as macrophages (1:200) (*12*) and the most motile ABP$^+$ cell line, M6 (1:140).

The elastic modulus, a measure of the shear stress needed to achieve a given deformation, of a pellet of intact cells from the ABP-transfected subline M2A7 was 657 ± 40 dynes/cm^2, more than twice that of the control M2 line (281 ± 10 dynes/cm^2), and similar to that of ABP$^+$ line M4 (750 ± 43 dynes/cm^2) (*13*).

Our results emphasize the importance of ABP as a gelation factor in mammalian cells. Restoration of ABP to deficient cells increased measurements of physical elasticity in vivo. Peripheral organelle exclusion, thought to be a function of interfilament pore size (*14*) became apparent. Blebbing of the plasma membrane, which has been ascribed to peripheral cytoskeletal instability (*15*), was prominent in cells lacking ABP and reduced when amounts of ABP were increased. Finally, ABP$^-$ cells had poor pseudopod protrusion and impaired motility, and this was similarly reversed after transfection.

ABP connects actin filaments to membrane glycoproteins as well as to each other (*16*) and may thereby provide surface stabilization by gelation of peripheral actin, ligation of the submembrane actin gel to the plasmalemma, or both. Because ABP$^-$ and ABP$^+$ cells responded with surface protrusive activity to stimulation by serum, the membrane signaling pathway appeared to be intact in both groups. However, the blebs seen in the ABP$^-$ cells involved the entire surface of the cell, rather than a localized area, implying that the inability of ABP$^-$ melanoma cells to localize their protrusive activity may be another aspect of their impaired migration. In addition, the efficiency of ABP in cross-linking actin filaments and possibly binding to membrane receptors may concentrate the ingredients for continuing protrusion in the initially stimulated region of the cell, despite signaling events in the membrane elsewhere.

The ABP$^-$ melanoma cells have an ABP gene, and ABP protein underexpression is the result of markedly reduced ABP mRNA levels, implying that regulation of ABP gene expression or mRNA stability causes the lack of ABP protein in ABP$^-$ cell lines. Melanoma can be a locally invasive cancer, and the locomotory efficiency of the tumor cells might influence tissue invasion and metastasis and thus the clinical course of the disease.

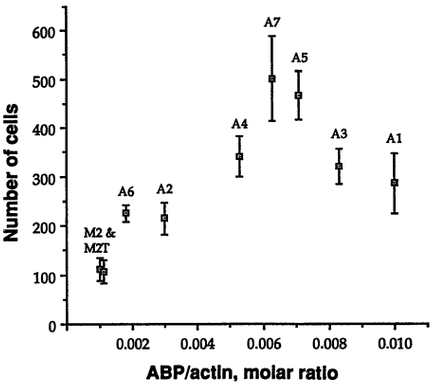

Fig. 3. Migratory ability of the ABP-transfected sublines as a function of the molar ratio of ABP to actin. Cells migrated in response to a gradient of conditioned medium. Error bars indicate SEM for at least eight determinations for each line.

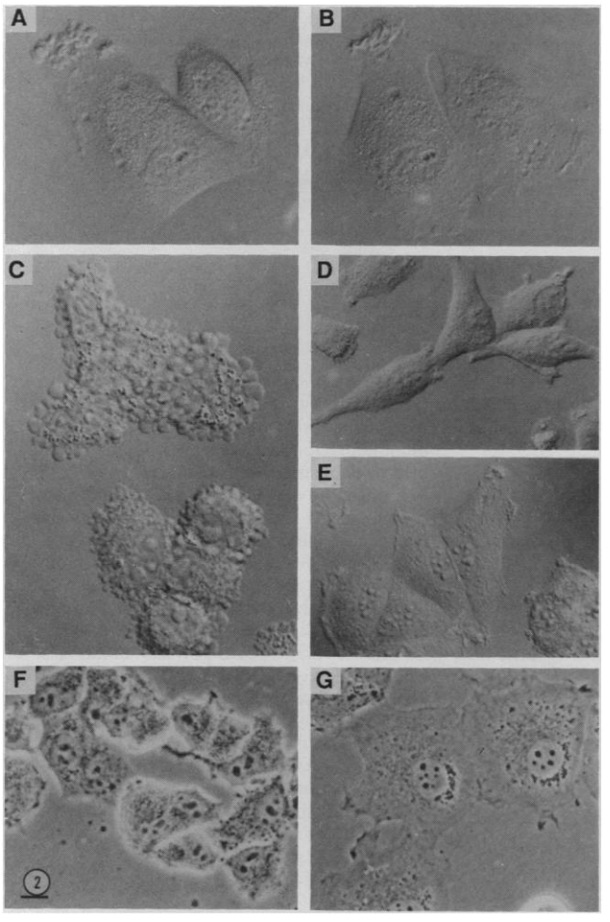

Fig. 2. Photomicrographs comparing surface activity in various cell lines. (**A** and **B**) DIC photomicrograph of an ABP$^+$ M5 cell with localized blebbing at the top left corner, which transformed to ruffling in the next frame taken 10 s later. ABP$^-$ M2 cells (**C**) with extensive surface blebbing in contrast to cells from the ABP-transfected sublines M2A5 (**D**) and M2A7 (**E**). Phase contrast photomicrograph of an M2 cell (**F**) showing lack of peripheral organelle exclusion compared to ABP-transfected subline M2A7 (**G**). The melanoma lines were grown in Minimum Essential Media (MEM) supplemented with newborn calf serum (8%), fetal calf serum (2%), and penicillin and streptomycin (100 units/ml) (Gibco-BRL, Grand Island, New York) at 37°C in an atmosphere containing 5% CO_2. Bar represents 20 μm.

REFERENCES AND NOTES

1. T. P. Stossel, P. A. Janmey, K. S. Zaner, in *Cytomechanics*, J. Bereiter-Han, O. R. Anderson, W. E. Reif, Eds. (Springer, Berlin, 1987) pp. 131–153.
2. T. P. Stossel, *J. Biol. Chem.* **264**, 18261 (1989); T. D. Pollard and J. A. Cooper, *Annu. Rev. Biochem.* **55**, 987 (1986).
3. M. Brink *et al.*, *J. Cell Biol.* **111**, 1477 (1990); M. Schleicher *et al.*, *J. Cell Sci.* **90**, 59 (1988).
4. J. H. Hartwig, J. Tyler, T. P. Stossel, *J. Cell Biol.* **87**, 841 (1980); J. H. Hartwig and T. P. Stossel, *J. Biol. Chem.* **250**, 5696 (1975). The name filamin was given to a protein structurally similar to ABP isolated from smooth muscle of chicken gizzard [K. Wang, J. F. Ash, S. J. Singer, *Proc. Natl. Acad. Sci. U.S.A.* **72**, 4483 (1975)], though this protein is less efficient in actin gelation, presumably because it does not allow wide-angle cross-linking of actin filaments [E. A. Brotschi, J. H. Hartwig, T. P. Stossel, *J. Biol. Chem.* **253**, 8988 (1978)].
5. J. Gorlin *et al.*, *J. Cell Biol.* **111**, 1089 (1990).
6. H. R. Byers, T. Etoh, J. R. Doherty, A. J. Sober, M. C. Mihm, *Am. J. Path.* **139**, 423 (1991).
7. Gelsolin and ABP were immunoprecipitated as reported (*17*). Immunoblotting was performed by standard methods with ^{125}I-labeled secondary immunoglobulin G (NEN, Boston, MA). Monoclonal antibodies were used to detect ABP (*5*), α-actinin [I. Virtanen, University of Helsinki; O. Narva-

nen, A. Narvanen, V. M. Wasenius, P. Partanen, I. Virtanen, *FEBS Lett.* **224**, 156 (1987)], and gelsolin (*17*). Polyclonal antibodies were used to detect profilin [J. H. Hartwig, K. A. Chambers, K. L. Hopcia, D. J. Kwiatkowski, *J. Cell Biol.* **109**, 1571 (1989)], and fodrin [J. Morrow, Yale University; A. S. Harris, L. A. Green, K. J. Ainger, J. S. Morrow, *Biochim. Biophys. Acta* **830**, 147 (1985)].

8. We obtained RNA from cells by the guanidinium isothiocyanate–cesium chloride method [J. M. Chirgwin, A. E. Przybyla, R. J. MacDonald, W. J. Rutter, *Biochemistry* **18**, 5294 (1979)] and quantitated it by measuring absorbance at 260 nm. Ribonuclease protection analysis of ABP message RNA was performed as described (*17*) with a 2.1-kb ABP cDNA (7) random oligonucleotide–labeled probe [A. P. Feinberg and B. Vogelstein, *Anal. Biochem.* **132**, 6 (1983)]. Southern blot analysis was done by standard methods using the 2.1-kb ABP cDNA to probe the membrane.
9. For videomicroscopy, cells were plated on a 25-mm glass cover slip and placed in a Leiden incubation chamber (Motion Analysis, Greenville, NY) at 37°C in an atmosphere of 5% CO_2. Differential interference contrast (DIC) microscopy was performed on a Zeiss Axiovert 405M inverted microscope with either a 40×, 0.9 numerical aperture (N.A.) Planneofluor objective or a 63×, 1.4 N.A. Planapochromatic objective. For time-lapse recordings, images were transmitted to a Hamamatsu 2400 videocamera and recorded on a Panasonic 6750AG video recorder.
10. Overlapping ABP cDNA clones were assembled into one complete construct in Bluescript SK+ (Stratagene) by standard methods and ligated to LK444, which contains the human β-actin promoter [P. Gunning, J. Leavitt, G. Muscat, S. Y. Ng, L. Kedes, *Proc. Natl. Acad. Sci. U.S.A.* **84**, 4831 (1987)]. The complete LKABP plasmid was transfected into the cells by calcium phosphate coprecipitation. After two days, the culture medium was replaced with medium containing G418 (1000 μg/ml) (Gibco-BRL, Gaithersburg, MD). Resistant colonies of cells were serially diluted into multiwell plates and cultured separately.
11. Medium in which cells from lines M1 to M6 were grown had both chemokinetic and chemotactic activity. The greatest stimulation of motility occurred with medium conditioned by M4 cells, so that medium was used in all subsequent assays. For motility assays, 5×10^4 cells were placed in each well of a 48-well, two-compartment chamber (Nucleopore, Pleasanton, CA) separated by an 8-μm pore size polycarbonate filter. To create a gradient of chemoattractant, conditioned medium was added to one of the chambers. After incubation (2 hours at 37°C), the filter was removed, stained, and examined with a 10× objective, and the number of cells that had migrated through the membrane was counted for each well.
12. J. H. Hartwig, in *The Lung: Scientific Foundation*, R. G. Crystal *et al.*, Eds. (Raven Press, New York, 1991) pp. 141–153.
13. The elastic modulus of a pellet of cells depends on the elasticity of the individual cell cortices in the same manner as measurements of continuous networks of micron size gels depend on the viscoelasticity of the individual microgels [H.-F. Eicke, C. Quellet, G. Xu, G. Riess, in *Physical Networks: Polymers and Gels*, W. Burchard and S. Ross-Murphy, Eds. (Elsevier, London, 1990), pp. 169–184] and can be measured in a torsion pendulum. Packed cells (400 μl) were applied to the bottom plate of a torsion pendulum [P. A. Janmey, *J. Biochem. Biophys. Methods* **22**, 41 (1991)]. Oscillatory measurements were begun one min later and continued for an hour. A constant shear stress was then applied for 10 min, during which time the displacement of the sample, quantitated as shear strain, was measured. The stress was then removed and the recovery of the sample toward its original undeformed state was measured. Oscillatory measurements were repeated after this experiment, and for all samples the value of G' measured was unchanged from that before imposition of the steady stress, confirming that the slow deformation did not alter the structure of the sample. The optical density and cell number were measured after all experiments, confirming that the samples contained approximately equal amounts of cell mass and that the cells remained rounded and intact during the measurements.
14. T. P. Stossel, *J. Cell Biol.* **99**, 15s (1984); K. Luby-Phelps, F. Lanni, D. L. Taylor, *Annu. Rev. Biophys. Chem.* **17**, 369 (1988).
15. E. Weiss *et al.*, *Beitr. Pathol.* **150**, 345 (1973); W. A. Davies and T. P. Stossel, *J. Cell Biol.* **75**, 941 (1977); D. A. Mesland, G. Los, H. Spiele, *Exp. Cell Res.* **135**, 431 (1981).
16. J. E. Fox, *J. Biol. Chem.* **260**, 11970 (1985); R. M. Ezzell, D. M. Kenney, S. Egan, T. P. Stossel, J. H. Hartwig, *ibid.* **263**, 13303 (1988); J. R. Okita *et al.*, *J. Cell Biol.* **100**, 317 (1985); Y. Ohta, T. P. Stossel, J. H. Hartwig, *Cell* **67**, 275 (1991).
17. D. J. Kwiatkowski, *J. Biol. Chem.* **263**, 13857 (1988).
18. We thank K. Weimer, M. DeSisto, and J. Lamb for technical help. Supported by NIH grants AI 08051 (C.C.C.), HL 19429 (T.P.S.), AR 38910 (P.A.J.), DK 38452 (J.H.H.), and HL 02158 (J.B.G.), and grants from the Whittaker Foundation and the Council for Tobacco Research. T.P.S. is an American Cancer Society Research Professor and D.J.K. is an Established Investigator of the American Heart Association.

15 July 1991; accepted 23 October 1991

Cyclic 2′,3′-Phosphates and Nontemplated Nucleotides at the 3′ End of Spliceosomal U6 Small Nuclear RNA's

ELSEBET LUND AND JAMES E. DAHLBERG

Spliceosomal U6 small nuclear RNA (U6 RNA) in species as diverse as man, frog, fruitfly, and soybean have at their 3′ ends a cyclic 2′,3′-phosphate (>p) apparently derived from uridylic acid residues that were added post-transcriptionally. The 3′ ends of U6 RNA's from various sources may be processed in different ways, or to different extents, depending on the organism or stage of development. The presence of a >p terminus on U6 RNA may influence the activity of U6 RNA either directly during splicing or indirectly by ensuring that the RNA has a defined length or proper conformation (or both).

U6 RNA, ONE OF FIVE SMALL NUclear RNA's (snRNA's) that function in pre-mRNA splicing (*1*), has several unusual characteristics that distinguish it from other snRNA's. It is synthesized by RNA polymerase III, rather than II, it lacks the Sm antigen binding site present in other spliceosomal snRNA's, and it has a methyl triphosphate at its 5′ end rather than a hypermethylated cap (*2, 3*). Mutational probing of U6 RNA has revealed that the 3′ terminal domain, extending from the region of interaction between U4 and U6 (*4*) to the 3′ end, is important for function (*5*). Alterations of the phylogenetically conserved length of this 3′ terminal domain decrease the activity of yeast U6 RNA in an in vitro splicing system (*6*). Also, base-pairing of sequences in this region with U2 RNA is essential for splicing in vertebrates (7), but not in yeast (*8*).

The major 3′ end sequence of mammalian U6 RNA is reported to be (5′) G-U-U-C-C-A-U-A-U-U-U-U-(U)$_{OH}$ (3′) (*9*). Like other RNA pol III transcripts that end with three to six U's (*10*), newly synthesized U6 RNA binds to the nuclear antigen La and is precipitated by antibodies to La (anti-La) (*11–13*). However, the major, mature form of U6 RNA (either free or complexed with U4 snRNA) is not precipitable by anti-La and it differs at its 3′ end in a hitherto undetermined way from the newly made U6 RNA (*11*). The sequence at the 3′ end of the RNA was deduced by labeling with pCp (*9*) or from U6 gene sequences (*14*), and therefore post-transcriptional alterations would have gone undetected. We show that the major 3′ end of U6 RNA contains a cyclic 2′,3′-phosphate (>p) end group, as opposed to the *cis* 2′,3′-diol end group of the anti-La precipitable U6 RNA's; this explains the lack of binding of mature U6 RNA to La antigen and reveals a novel feature of RNA metabolism.

In mammalian cells, the size of the steady-state population of U6 RNA's is heterogeneous, and multiple forms can be detected by RNA blot analysis (*15*), the most abundant form having the fastest mobility (Fig. 1A, lane 1). Some of this heterogeneity could be attributed to maturation of U6 RNA because the gel mobilities of newly made ^{32}P-labeled U6 RNA's increased with time (lanes 2 and 3) (*16*). Although this trend would be consistent with a shortening of the RNA during maturation, direct nucleotide sequence analyses (Fig. 1B) indicated that the mature U6 RNA (lane 3) was actually longer than the newly transcribed U6 RNA (lane 2).

RNase T1 fingerprint analyses (*17, 18*) of U6 RNA's made in vivo showed that the 3′ ends of U6 RNA's changed with time (Fig. 1B); this alteration might account for the inability of mature U6 RNA to bind La

Department of Biomolecular Chemistry, University of Wisconsin Medical School, 1300 University Avenue, Madison, WI 53706.